Innovative thermal and acoustic insulation foam from recycled waste glass powder

Giada Kyaw Oo D'Amore [a], Marco Caniato [a, *], Andrea Travan [b], Gianluca Turco [c], Lucia Marsich [a], Alessio Ferluga [a], Chiara Schmid [a]

[a] Engineering and Architecture Department, University of Trieste, Italy
[b] Life Science Department, University of Trieste, Italy
[c] Department of Medicine, Surgery and Health Sciences, University of Trieste, Italy

ARTICLE INFO

Accepted 28 July 2017

Keywords:
Waste reuse
Sound absorbing foam
Glass powder
Alginate

ABSTRACT

An innovative powder-foaming process able to produce thermal and acoustic insulating foams obtained by sol-gel and a subsequent freeze-drying process was developed.

Gel containing glass powder was formed using alginate, a polysaccharide composed of 1-4linked α-L-guluronic acid and β-D-mannuronic acid, capable to form stable gels in presence of calcium cations. In order to obtain a porous foam, gels were frozen and then freeze-dried. Foam properties strongly depend on production parameters, particle dimension and different binder concentrations, their influence was investigated. The resulting glass foams were characterized in order to evaluate structure, density, mechanical and acoustic properties. The results pointed out an improved acoustic insulating performance respect to rock wool.

Foams were also subjected to a thermal process to better fix powders into the final glass structure.

1. Introduction

Nowadays, the increased awareness of environmental issues, waste material reuse and new eco-compatible products manufacturing, led the European Commission to set targets to promote municipal waste recycling up to 65% and to reduce landfill to a maximum of 10% by 2030 (European Commission, 2017). The lack of efficient and cost-effective recycling technologies requires novel strategies (i.e. energy efficiency protocols as demonstrated by Caniato and Bettarello, 2013, rewarding use of recycled materials etc.) able to recycle materials which are actually landfilled. Tons of glass wastes are generated every year worldwide; a huge percentage of them is composed of a mixture of pieces with a wide range of particle sizes and colours. Moreover, glass can be contaminated with metallic and non-metallic fragments. The use of this mixture in new material manufacturing is not recommended since the final products will have poor quality and, on the other hand, colour sorting and impurity removal are expensive (Scarinci et al., 2005). Glass waste incineration creates problems because the solid residue could contain hazardous materials (Colombo et al., 2003)-. Several studies have highlighted the benefit from adding small particles of glass cullet in the production of ceramics, compact or compacted layers, bricks (Bettarello et al., 2010a; Di Monte et al., 2013; Omran and Tagnit-Hamou, 2016; Parghi and Alam, 2016) or glass foams. Foam production from glass waste is a good way to save landfill costs and reuse different types of glass (*e.g.* waste soda-lime glass or industrial residues from the manufacturing of glass fibers) in different size (Bernardo et al., 2010). For this application, the glass wastes commonly employed are mixed-colour bottle glass (Gong et al., 2016) and window glass (Fernandes et al., 2009; Granzotto et al., 2017), but other type, such end of life fluorescent lamp (EOLFL) glass as demonstrated by Mugoni et al. (2015), cathode ray tubes (CRTs) as showed by Singh et al. (2016) and vitrified solid residual from municipal waste combustion (König et al., 2016), can also be used.

In literature, glass foams are reported to be lightweight, compression-resistant, thermally insulating, sound absorbing or insulating for both airborne or impact noise (Caniato et al., 2015, 2016a; Bettarello et al., 2010b), non-flammable and water and steam resistant. In addition glass foams exhibit several advantages over conventional insulating materials (*e.g.* mineral wool): they provide (i) freeze-thaw tolerance, (ii) excellent chemical and

* Corresponding author.
E-mail address: mcaniato@units.it (M. Caniato).

thermal stability, (iii) high surface area and permeability, (iv) superior mechanical properties and (v) a lifespan much longer than conventional thermal insulating materials. Due to their unique properties, glass foams could have several applications such as acoustic and thermal insulation, catalyst supports, lightweight aggregate materials in concrete and biomedical implants (Qu et al., 2016).

At present, two industrial processes for glass foams production exist; the former dates back to 1930 and requires fluid blowing (*e.g.* air, CO_2 or water vapour) directly into the molten raw materials (Lyttle, 1940). The costs related to the high energy consumption to prepare the glass melt represent the main drawback of this method. Bernardo (2007) substituted it by a process at lower temperature, combining foaming and sintering process.

Nowadays, the main industrial processes mix glass powders with suitable blowing agents using for example $CaCO_3$, $MgCO_3$ (Bernardo et al., 2010; Fernandes et al., 2014), Na_2CO_3, SiC or organic compounds (Fernandes et al., 2009; Hasheminia et al., 2012; Andreola et al., 2016a), high temperature promotes blowing agents decomposition (Andreola et al., 2016b) or oxidation (Ketov, 2003), allowing the release of gases and the consequent pores creation in the final sintered glass structure (Bernardo and Albertini, 2006). Conversely the production costs, mainly due to high temperature, limit glass foams market (Bernardo et al., 2007). Foams properties strictly depend on temperature process, foaming agent and particle size, which also influences final product density and homogeneity.

To the best of our knowledge, foaming methods characterized by low temperatures and without blowing agents employment are currently unavailable. The aim of this study is to develop and characterize an innovative acoustic insulating foam produced using glass waste and realized by a freeze-drying process. This target was achieved through the incorporation of recycled glass powder in an alginate matrix. In this paper, this novel patent pending approach to manufacture glass-alginate composites is devised and the resulting freeze-dried foams are characterized in terms of morphological, mechanical and acoustic properties.

2. Materials and methods

Glass powder used to produce foams was obtained by grinding old laboratory glassware (beakers) made of borosilicate glass with a Herzog mill with iron jar (typical composition of Pyrex borosilicate glass: SiO_2 80,6%, B_2O_3 13.0%, Na_2O 4.0%, Al_2O_3 2.3%, others 0.1%). Even though cation leaching from the glass is unlikely under the mild reaction conditions here employed (Terribile et al., 1999), mostly calcium-free borosilicate glass was preferred to avoid any possible interference with the gelling medium (Ca^{++}).

Alginic acid sodium salt from brown algae (medium viscosity), D-Gluconic acid δ-Lactone (GDL, ≥99.0%) and $CaCO_3$ (98%, particle size $\leq$ 30 μm) necessary for the sol-gel process were purchased from Sigma Aldrich.

2.1. Glass particle size analysis

Glass particle size analysis was performed on five samples according to ISO 13320 (2009), using a laser granulometer Master Size 2000E of Marvel Instrument. Demineralized water was used as dispersing liquid; the glass powders had a concentration of about 15%w/v. Data were processed according to the Mie theory (Gouesbet and Grehan, 2011) and the refractive index of Flint glass (Batsanov et al., 2016) was employed.

2.2. Preparation of foam samples

Foam production process was carried out according to a patent pending procedure devised by some of the authors (Caniato and Travan, 2016).

The method was based on the preparation of a glass-alginate composite hydrogel, which was then freeze-dried. The principle of synthesis route was based on the initial formation of a three dimensional porous hydrogel network which structure was preserved by freeze-drying, a process that avoid the presence of liquid water and the consequent pores collapse (Zhang and Khademhosseini, 2017). Cells were formed because of the hydrogel structure freeze-drying process: the water entrapped during gelation was removed by sublimation during the freeze-drying procedure, obtaining a porous structure. The glass powder (with final concentration from 5 to 20%w/v) was dispersed in alginate aqueous solution (with final concentration from 1 to 1.7%w/v) and the *in situ* gelation approach was followed (Travan et al., 2009, 2016; Marsich et al., 2013). The gelation of alginate-based solutions occurred because calcium ions were able to bind (preferentially) to the G-blocks of the polysaccharide in a highly cooperative manner, resulting in ionic crosslinking. In particular, with the *in situ* gelation approach, calcium ions were slowly released from $CaCO_3$ when the pH of the aqueous solution gradually decreased as a consequence of GDL hydrolysis in water. $CaCO_3$ and glucono delta-lactone GDL were used at final concentrations of 20−40 mM and 40−80 mM, respectively.

The concentrations of alginate, $CaCO_3$ and GDL were selected on the basis of the following criteria. Before addition of calcium ions, the viscosity of the alginate-glass suspension should enable proper stirring while allowing a homogeneous dispersion of the glass powder within the polymer solution: this was experimentally optimized by employing alginate concentrations in the range of 1−1.7%w/v. Lower alginate values could not ensure a sufficient viscosity to sustain glass particles, while higher alginate concentrations resulted in excessive viscosity of the slurry. The concentrations of $CaCO_3$ and GDL were typically employed in the *in situ* approach to ensure a homogeneous and gradual crosslinking of alginate solution. When the amount of GDL was increased, a faster crosslinking occurred; this was exploited to avoid possible gravity-driven sedimentation of the glass powder during the gelation process. Petri dishes with a diameter of 90 mm were used to obtain gels with final volume of 52.8 mL. The concentrations used for each type of sample are listed in Table 1. After 12 h, gels were frozen at −80 °C and finally freeze-dried.

2.3. Density

A Gay-Lussac pycnometer was used to determinate the glass powder density, according to ISO 3507 (1999). Tests were performed on three samples.

Table 1
Identification of produced samples.

Sample code	Alginate [%w/v]	$CaCO_3$ [mM]	GDL [mM]	Glass [%w/v]
1	1	20	40	5
2	1.5	20	40	5
3	1.5	20	40	10
4	1.5	20	40	20
5	1.5	20	80	10
6	1.5	20	80	20
7	1.7	20	40	10
8	1.7	20	40	20
9	1.7	20	80	10
10	1.7	20	80	20

The foam apparent density was determined from mass and dimensions of three samples.

2.4. Thermal characterization

A heating microscope Misura® HSM was used for the thermal analysis of glass powder in order to identify the softening and the sintering temperatures. Cylindrical samples (2 × 3 mm) of glass powder (18 mg) were prepared and heated from room temperature (27 °C) up to 850 °C, with a heating rate of 10 °C/min. The microscope was programmed to take pictures every 2 °C. The test was repeated three times on three different samples in order to ensure result reproducibility.

Simultaneous thermal analysis (STA) was performed using a Netzsch STA 409 EP with alumina crucibles. The tests were done using about 30 mg for both glass foams and raw alginate, with a heating rate of 10 °C/min in dynamic air (flow rate 2 mL/min) from 20 to 800 °C.

2.5. Freeze-drying and thermal treatment

Freeze-drying was implemented in an Alpha 1–2 LD Plus freeze drier, connected to a vane pump (Vacuubrand RZ 2.5).

Some foam samples were thermally treated in order to consolidate glass particles.

A laboratory furnace Linn High Therm Germany VMK 1800 was used; different cycles in terms of temperature and time were tested as reported in Table 2.

2.6. Microscope and image analysis

Foam macrostructure was analysed with two optical microscopes, a Nikon SMZ 2T for magnifications up to 6.3x and a Nikon Optiphot for superior magnifications.

Foam microstructure was analysed using a Leica-Stereoscan 430i Scanning Electron Microscope (SEM). Samples were sectioned and visualized by SEM after Au sputter coating.

Image J software was used for image analysis.

2.7. Acoustic properties

Acoustic properties on polymers could be performed using different techniques as showed by Caniato et al. (2016b).

In this case study, sound absorption analysis was performed with a Kundt tube with a diameter of 45 mm according to ISO 10534 (1998). Tests were performed on three samples of 10 mm thickness and on three 80 kg/m^3 rock wool samples of same thickness.

The sound absorption coefficient (α) indicates sound fraction absorbed by the material. The absorption coefficient provided by the data acquisition system is expressed as:

$$\alpha = I_a / I_i$$

where

I_a = absorbed sound intensity (W/m^2)
I_i = incident sound intensity (W/m^2)

2.8. Compression tests

Compression tests were performed with a Shimadzu Autograph 2, AG-10TA equipped with a 500 N load cell. A constant compression speed of 2.5 mm/min was used according to the ASTM D1621 (2010) and the compression modulus E_c was determined from the load-displacement curves: deformation could be considered linear from 0.03 to 0.08 mm. Tests were performed on five specimens with an average diameter of 28.9 mm and an average height of 25.4 mm.

3. Results

3.1. Gelation process

The rationale of this study was to devise an innovative environmentally-friendly approach to manufacture insulating porous material starting from recycled glass and water-soluble polymers obtained from renewable sources (seaweeds). The proposed method was based on two main steps: i) incorporation of glass powder in a polysaccharide-based hydrogel, ii) water sublimation through a freeze-drying process to preserve the intimate structure of the hydrogel, leading to a highly porous system. In addition some samples were also subjected to a thermal treatment to allow glass particles sintering and polymer scaffold decomposition. Preliminary studies were performed to set processing parameters in order to attain homogeneous hydrogels and foams. Samples 1 and 2 were necessary to demonstrate that the process produced a porous structure, but these foams were difficult to handle since they were very brittle. Samples with a GDL concentration lower than 80 mM (3, 4, 7 and 8) showed problems of glass powder precipitation. Only the results of samples 6 and 10 were reported because the optimization of the higher waste concentration in the final product was preferred.

Fig. 1 shows an example of the glass foam manufactured with the above described process. It is possible to note the porous structure created by the freeze-drying process.

3.2. Glass particle size analysis

In Fig. 2 the average distribution of glass particle size is reported. It is possible to observe that approximately the 50% of the particles

Table 2
Thermal cycle's description.

Code	Heating rate [°C/min]	Maximum T [°C]	Plateau time [min]	Cooling rate [°C/min]	Intermediate T [°C]	Plateau time [min]	Cooling rate [°C/min]
A	10	750	30	furnace	/	/	/
B	10	750	90	furnace	/	/	/
C	10	800	30	furnace	/	/	/
D	10	800	30	5	680	30	furnace
E	10	750	90	5	680	30	furnace
F	10	800	30	5	680	60	furnace
G	10	650	30	furnace	/	/	/
H	10	650	20	furnace	/	/	/
I	10	630	30	furnace	/	/	/
L	10	640	20	furnace	/	/	/

Fig. 1. Example of not-sintered glass foam and a macro structure detail (sample 10).

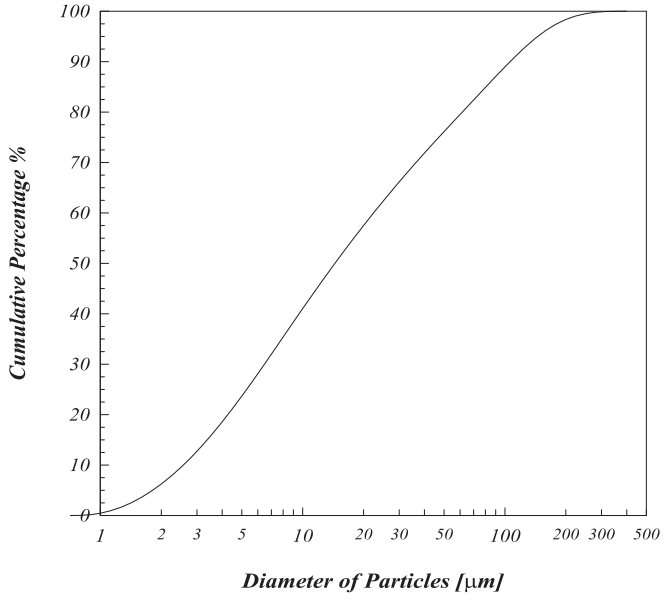

Fig. 2. Glass particle size distribution.

has a size lower than 16 μm.

3.3. Glass powder thermal behaviour

In Fig. 3 the results obtained with the heating microscope are reported. The software determines automatically the characteristic temperatures: at the sintering point (676 °C) the sample reaches a dimensional variation corresponding to a defined percentage referring to the first image acquired, considered as 100%; at the softening point (800 °C) sample corners starts toround and the wall becomes smooth. Characteristic temperatures evaluation was performed considering sample height at the beginning (100%), after reduction of 5% (sintering point, 95% of initial height) and after reduction of 17.5% (softening point, 82.5% of initial height). Temperatures were defined and identified according to the highly reliable Misura™ standard (TA intruments/Waters LLC, Misura 4.0.16 Documentation). Anyway, from Fig. 3, it is evident that sample starts shrinking at 627 °C.

These results were applied to determine the thermal cycles used during foam sintering.

3.4. Glass powder and foam density

The glass powder used to produce foams had a density of 2.63 g/cm^3. Glass foam samples 6 and 10 (not-sintered) had a density of 0.186 ± 0.025 g/cm^3 and 0.201 ± 0.016 g/cm^3 respectively. The small difference between samples can be explained by slightly different synthesis conditions and the use of a “hand-made process”.

3.5. Thermal analysis (STA)

In Figs. 4 and 5, TG and DTA curves of raw alginate and not-sintered glass foam are reported. In Fig. 4, it is possible to observe that after dehydration (first endothermic peak on the DTA curve), the alginate decomposition proceeds with two exothermic steps (first step at 240 °C and second step at 360 °C in agreement with literature as reported by Soares et al., 2004) with an overall weight

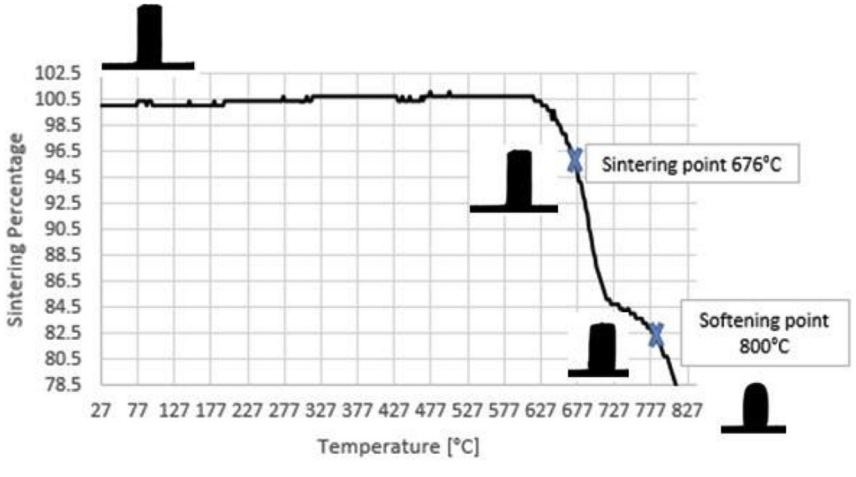

Fig. 3. HSM analysis's plot reporting sintering and softening temperatures.

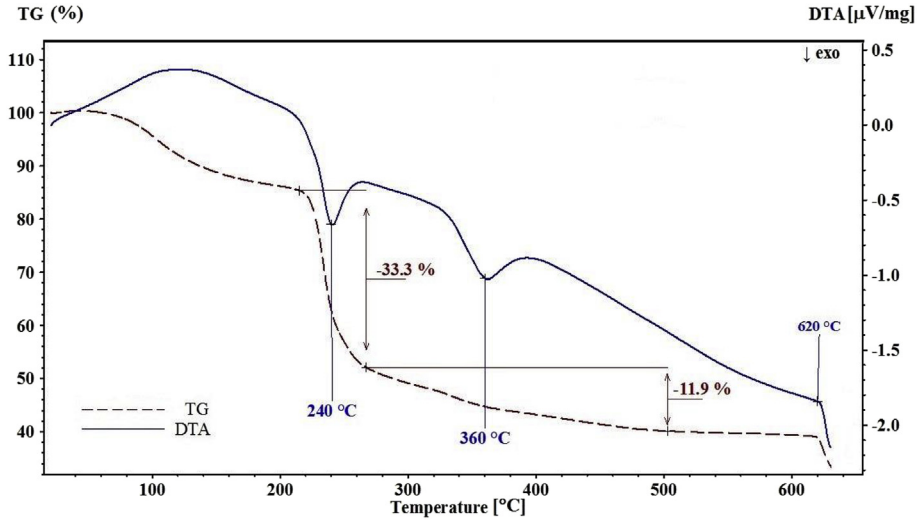

Fig. 4. TG and DTA curves of raw alginate.

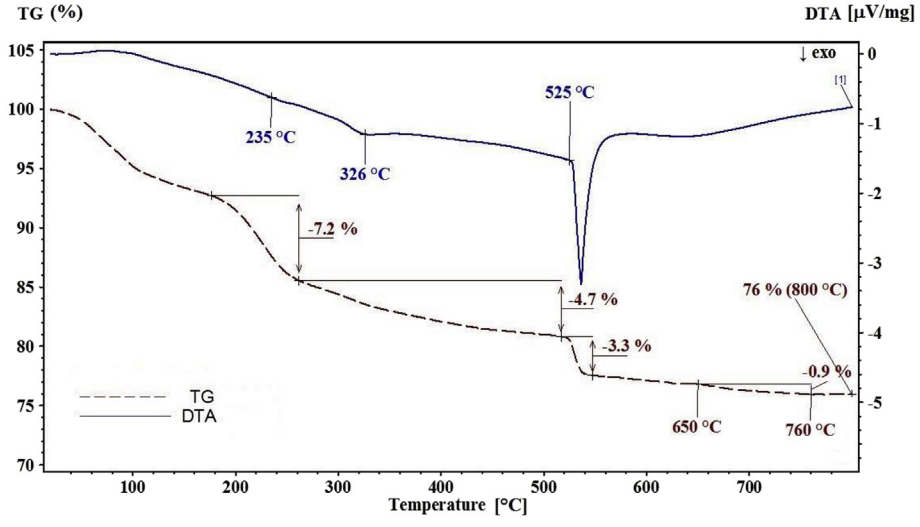

Fig. 5. TG and DTA curves of not-sintered glass foam.

loss of 61%. Final oxidation starts at 620 °C.

The thermal behaviour of the not-sintered foam is quite different (Fig. 5). Only the two steps belonging to alginate decomposition are visible: the first at 235 °C and the second at 326 °C, lower than the temperature measured for raw alginate. Alginate oxidation starts at lower temperature (525 °C versus 620 °C of the raw alginate). At about 650 °C the $CaCO_3$ decompose and at 800 °C the final residual mass composed by glass and CaO is 76%wt.

3.6. Sound absorption

Fig. 6 reports the average sound absorption coefficients α as a function of the frequency of not-sintered samples 6 and 10. Results are compared with rock wool average sound absorption coefficient.

Frequencies lower than 100 Hz are not reported since their absorption strongly depends on sample thickness and results are not significant. It can be noted that in the medium-high frequency range (typical of voice as reported by Caniato et al., 2013, 2016d; Caniato et al., 2016c) the sound absorption glass foam is higher than rock wool. This behaviour is related to the different porous

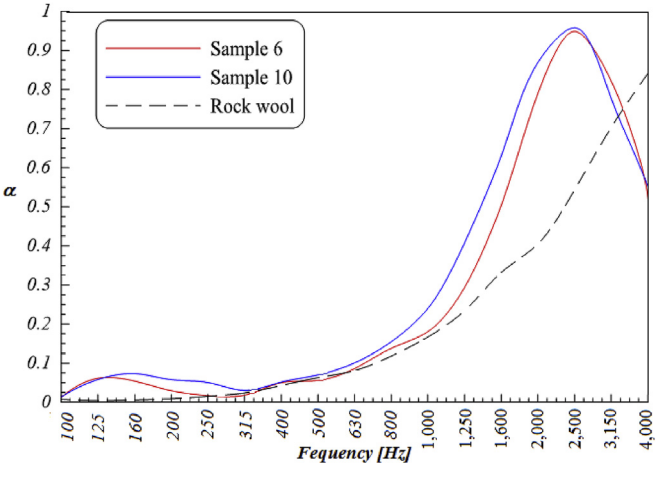

Fig. 6. Average sound absorption coefficients of not-sintered samples 6 and 10 compared with rock wool.

structure of materials:since the foam has an open cell structure, it gains the best performancein the range from 1250 Hz to 3150 Hz consistent with, as an example, polyurethane and melamine (Allard and Atalla, 2009; Doutres et al., 2010; Bonfiglio and Pompoli, 2016). Bonfiglio and Pompoli (2007) highlighted that the tortuosity changes the sound absorption properties passing from an open cell structure to a fibrous one.

3.7. Uniaxial compression test

In Fig. 7, the average load-displacement curves of not-sintered samples 6 and 10 are reported.

The compression tests were stopped before samples breakage, since they did not show a sudden failure. Cell structure underwent to a continuous crushing under load causing sample progressive compaction. The calculation of foam compression modulus was more significant:the average compression modulus and the standard deviation of not-sintered samples 6 and 10 were 5.2 ± 0.58 MPa and 4.2 ± 0.25 MPa.

3.8. Thermal treatment

The thermal treatment (sintering) was performed in order to consolidate the glass particles incorporated into alginate cell walls. Bigger particles could not be completely trapped in the alginate matrix (as shown in Fig. 9) and might be released during handling.

Following thermal analysis results (Section 3.2 and 3.4), some thermal cycles for sintering process were selected (Table 2). Thermal cycles were changed during manufacturing depending on results obtained in terms of texture and macrostructure of sintered foams.

In order to define the best thermal treatment relative to sintered structure morphology, the attention was focused only on samples 2, 5, 6, 9 and 10, which were undergone to different heating cycles as reported in Table 3. The best result was obtained with cycle I.

The image analysis performed on samples 6 and 10 highlighted that, after sintering, samples had dimensional contraction up to 15%, caused by alginate matrix decomposition and glass particles shrinkage.

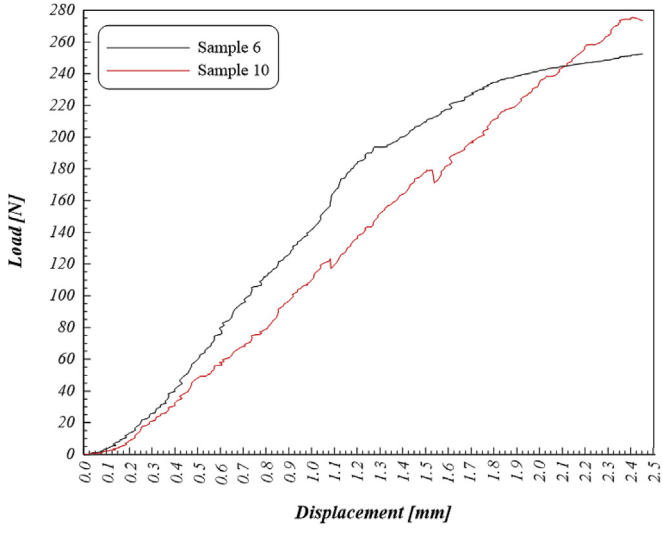

Fig. 7. Average load-displacement curves until 10% deformation of not-sintered samples 6 and 10.

Table 3
Types of thermal cycles for different samples.

Sample	Heating cycle applied
2	A → G
5, 9	F → L
6, 10	G → L

3.9. Scanning Electron Microscope

Glass foam microstructures before and after sintering process are reported in Figs. 8–11 respectively. In Fig. 8a) and b) it is possible to notice open cell structure in foam cross section; Fig. 9a) and b) show the particles distributed on alginate crosslinked branchescreated on the top of the sample; in Fig. 10a) and b) the cross section of sintered foams are reported. It can be noted that the structure is still porous. In Fig. 11 a) and b), a cross section is reported highlighting glass particles sintering necks; alginate walls disappeared.

4. Discussion

This study focused on the production technique of an innovative porous glass foam by means of a freeze-drying process; the procedure did not require high temperatures, chemical pollutants and any toxic gases were released. The alginate is a biopolymer with a neutral CO_2 balance and water used for gel formation was totally recovered.

The energy consumption of the presented process was calculated on the basis of electricity absorbed by laboratory equipment. A typical thermal cycle proposed in literature to produce glass foam was reproduced in laboratory and the power consumption was measured for comparison. The following Table 4 and Table 5 summarize the obtained data.

It is possible to conclude that on laboratory scale the presented process is cheaper than those founded in literature.

The freeze-dry process is a well known industrial practice, particularly in the food and pharmaceutical industry even for large volume production (Liapis and Bruttini, 2015). From the energetic point of view, freeze-drying is a more intensive process compared to conventional drying; however, this evaluation does not consider the high temperature step of the conventional foam production available on the market. Considering that (i) the hydrogel network could be reinforced to improve the mechanical properties and (ii) the new foam could be easily cut or formed, the suggested process appears as highly flexible as industrially cost-effective. For comparison, the commercial aerogel based insulating materials - such as those produced by Aspen Aerogels - include a supercritical drying step under batch condition in the production process. Finally, Life Cycle Assessment (LCA) of such process is environmentally favourable (waste recycling, mild process temperature, very low CO_2 emissions, etc.) and the products so obtained could be used in sustainable constructions (Caniato et al., 2017a; Caniato et al., 2017b).

The preliminary tests (samples 1 and 2) showed that with this method it is possible to form a cellular structure. Cell morphology is strongly anisotropic due to intentional uncontrolled gel freezing.

It was observed that components concentration affected foam performances. The lower GDL concentration (samples 3, 4, 7 and 8) caused problems of glass powder precipitation; this behaviour could be ascribed to slow gel formation, due to the slow release of calcium ions, which led particles to precipitate.

The glass percentage influences foam density which is lower for samples having 10% of glass powder (samples 5 and 9) than for

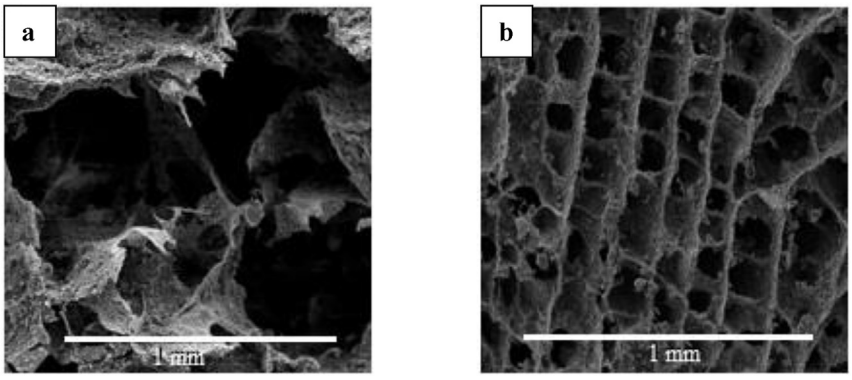

Fig. 8. Before sintering cross section; a) Sample 6; b) Sample 10.

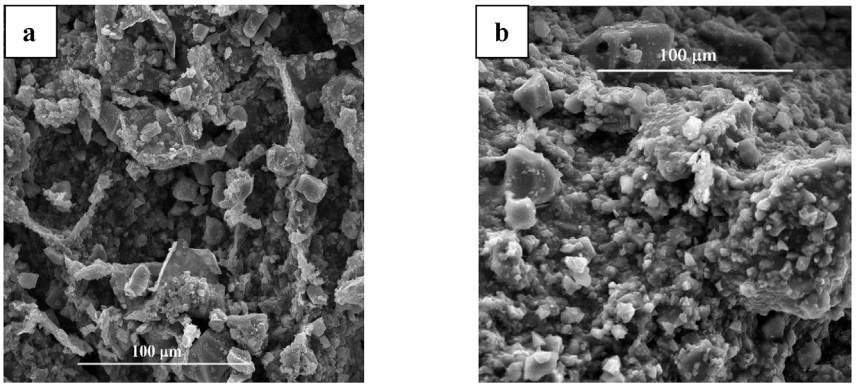

Fig. 9. Before sintering top view; a) Sample 6; b) Sample 10.

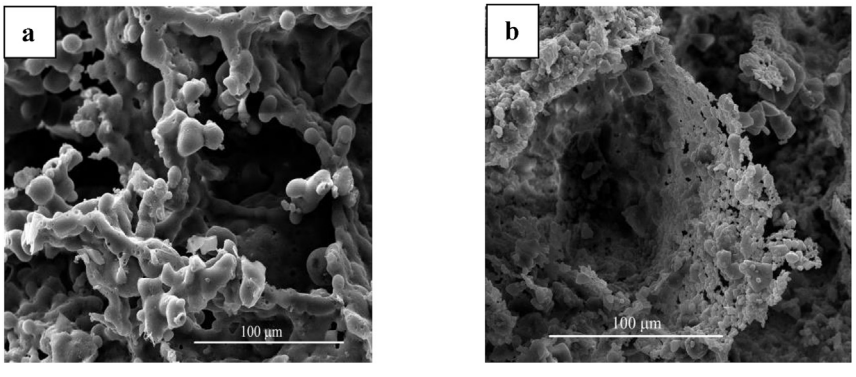

Fig. 10. After sintering (thermal cycle I) cross view; a) Sample 6; b) Sample 10.

samples with 20% (samples 6 and 10). However the lower glass concentration induces a higher dimensional shrinkage after sintering, without altering compressive strength and sound absorption coefficient.

Since the optimization of higher waste concentration in the final product was preferred, the study was focused only on foam with 20% of glass powder.

To limit the final foam density, the concentrations of alginate and glass were restricted to the values tested in this study.

STA results highlighted that alginate foam decomposition and oxidation temperatures are lower than for raw alginate; these temperatures decrease probably because the alginate is not in a massive form, but it is organized in thin leaves (foam walls), with a higher surface prones to oxidation. Moreover, considering the organic matrix decomposition temperature obtained by means of STA, the sintered foam (heat treatment at 630 °C) does not contain any longer the organic matrix.

Alginate content influences pore dimensions: a higher concentration (sample 10) leads to a smaller pore size and to a relatively higher density. SEM pictures highlight that sample 10 has a more compact structure (Fig. 8b) than sample 6, characterized bya lower alginate content (Fig. 8a).

The mechanical properties are consequently influenced: sample 6 alginate concentration equal to 1.5% has a higher compressive modulus than sample 10 (1.7%). Since sample 10 macrostructure is more compact it should be more rigid even if the foam density is quite similar and the pore size is smaller: this can be attributed to thinner and less resistant cell walls.

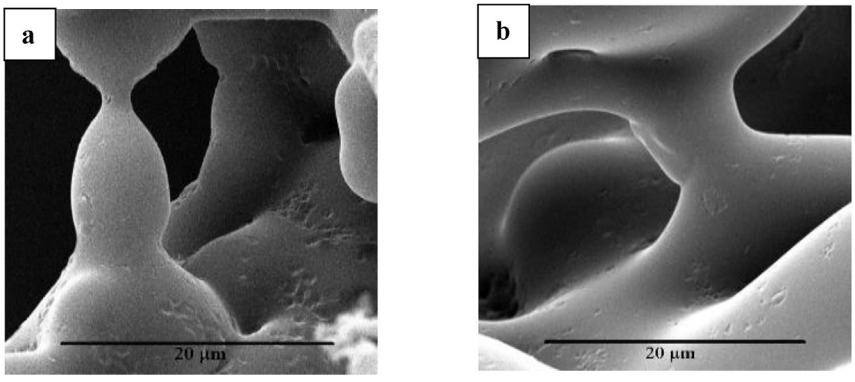

Fig. 11. After sintering (thermal cycle I) sintering neck; a) Sample 6; b) Sample 10.

Table 4
Presented foaming process.

	Medium industrial energy price [€]		freeze-drying (23 h, 8% of power)	vacuum pump (23 h, 40% of power)	tot
	0.15				
	freezer (5 h, 80% of power)	freeze-dryer and vacuum pump (0.5 h to achieve the required pressure and temperature, 100% of power)			
kWh	2.00	0.69	2.21	1.66	6.55
cost [€]	0.30	0.10	0.33	0.25	0.98

Table 5
Literature foaming process.

	Medium industrial energy price [€]		Cooling up to 700 °C at 5 °C/min (100% of power)	Oven at 700 °C (30 min, 8% of power)	tot
	0.15				
	Oven heating up to 1000 °C at 10 °C/min (100% of power)	Oven at 1000 °C (30 min, 8% of power)			
kWh	6.00	0.16	1.33	0.16	7.65
cost [€]	0.90	0.02	0.20	0.02	1.15

From the acoustic point of view, Papadopoulos (2005) reported that rock wool was choosen as reference because it is the most commonly applied insulating material in Europe. Compared to rock wool, foam exhibits a higher acoustic performance, especially at the medium-high frequencies, as clearly visible in Fig. 6. This behaviour is due to foam anisotropy and tortuosity and it also depends on cell size which is function of alginate content.

These properties could be useful for inner space acoustic retrofit as well as for sound insulation effects within airgap. The higher acoustic properties could permit to reduce panels thickness, allowing reduction of dimensions, weights and transportation costs.

The results obtained with the two selected samples permit to draw some observations, compared to glass foam (or other porous/fibrous like materials), since it starts from the same "raw material" and from the same initial issue: how to recycle glass powder.

In addition to the excellent acoustic properties, the foam does not release dust or fibres; this is a considerable advantage for operators health compared to other insulating materials handling (*e.g.* mineral or glass wool).

The new material can also behave as a thermal insulator, considering the small cell microstructure (Fig. 8b) capable to provide low thermal conductivity (Gwon et al., 2016; Wu et al., 2007). Since acoustic properties (Fig. 6) are very similar to those observed for polyurethane and melamine foam, it could be assumed that also thermal conductivity would be comparable.

Since glass foam final properties also depend on glass characteristics, such as glass type and particle size, there is the possibility to modulate the foam performance by varying these parameters.

The sintering process applied on some foam compositions was performed with the purpose to obtain a foam composed only by glass and to reduce glass particle loss from the surface. Indeed, with a thermal cycle at 630 °C for 30 min, the alginate matrix completely disappeared and the glass particle sintered (Fig. 10). On the other hand, since the final sintered foam is brittle and not easy workable, it was not characterized from acoustic and mechanical point of view.

5. Conclusions

This study describes an innovative method to produce glass foams. The production process advantages compared with those reported in literature are: (i) no need of high temperature, but the use of modulating pump with a lower energy consumption; (ii) the absence of chemical pollutants and toxic gases, in accordance with the provisions of the Europe 2020 Strategy; (iii) water used for gel formation recovery; (iv) additives with neutral CO_2 balance and completely biodegradable. The above mentioned features imply a

low carbon footprint.

Tests highlighted that with this method it is possible to form a cellular structure. Glass waste with small particle size, with different colours and impurities can be reuse in the manufacturing process, reducing polluting powders going to landfill. The final product is also recyclable at the end of its life. Synthesis conditions affect foam performances, since lower GDL concentration causes powder precipitation in the final sample.

The innovative glass foam could represent a viable alternative to rock wools thanks to its superior performance as acoustic insulator. This permits to reduce dimensions, weights and costs, referring to high CO_2 savings, very little waste (water without chemical additives and recoverable) and power saving using low temperatures and modulating pump. Contrary to rock wool, glass foam does not release fibres with a great advantage for operator health and environment. The glass percentage influences the final foam density, but lower glass concentration implies higher dimensional shrinkage.

Acoustics test and SEM analysis pointed out an open cell structure improving sound absorption in the medium frequency range as well as thermal insulation properties.

Author contributions

All authors contributed equally to the conception of this study.

Acknowledgement

The authors would like to thank Lorenzo de Lorenzi for his precious help for glass powder grinding, granulometry and density measurements.

The authors would like to thank prof. Jan Kaspar for his precious comments and suggestions.

References

Allard, J.F., Atalla, N., 2009. Propagation of Sound in Porous Media: Modelling Sound Absorbing Materials. Wiley.

American Society for Testing and Materials, 2010. Standard Test Method for Compressive Properties of Rigid Cellular Plastics. ASTM D1621– 16.

Andreola, F., Leonelli, C., Manfredini, T., 2016a. Recycling of industrial wastes in ceramic manufacturing: state of art and glass case studies. Ceram. Int. 42, 13333–13338. http://dx.doi.org/10.1016/j.ceramint.2016.05.205.

Andreola, F., Barbieri, L., Lancellotti, I., 2016b. Valorization of tyres waste pyrolysis residue in lightweight materials. Env. Eng. Manag. J. 15 (9), 1907–1914.

Batsanov, S.S., Ruchkin, E.D., Poroshina, I.A.P., 2016. Refractive Indices of Solids. Springer, Singapore.

Bernardo, E., 2007. Micro- and macro-cellular sintered glass-ceramics from wastes. J. Eur. Ceram. Soc. 27, 2415–2422. http://dx.doi.org/10.1016/j.jeurceramsoc.2006.10.003.

Bernardo, E., Albertini, F., 2006. Glass foams from dismantled cathode ray tubes. Ceram. Int. 32, 603–608. http://dx.doi.org/10.1016/j.ceramint.2005.04.019.

Bernardo, E., Cedro, R., Florean, M., Hreglich, S., 2007. Reutilization and stabilization of wastes by the production of glass foams. Ceram. Int. 33, 963–968. http://dx.doi.org/10.1016/j.ceramint.2006.02.010.

Bernardo, E., Scarinci, G., Bertuzzi, P., Ercole, P., Ramon, L., 2010. Recycling of waste glasses into partially crystallized glass foams. J. Porous Mater. 17, 359–365. http://dx.doi.org/10.1007/s10934-009-9286-3.

Bettarello, F., Caniato, M., Monte, R.D., Kaspar, J., Sbaizero, O., 2010a. Preliminary acoustic tests on resilient materials: comparison between common layers and nanostructured layers. In: 20th Int. Congr. on Acoust. 2010, ICA 2010-Incorporating Proc. of the 2010 Annual Conf. of the Australian Acoust. Soc. Volume 2,, Pages 1096-1101, Sydney, NSW; Australia; 23 August 2010 through 27 August 2010. Code 93749.

Bettarello, F., Fausti, P., Baccan, V., Caniato, M., 2010b. Impact sound pressure level performances of basic beam floor structures. Build. Acoust. 17 (4), 305–316. http://dx.doi.org/10.1260/1351-010X.17.4.305.

Bonfiglio, P., Pompoli, F., 2007. Frequency dependent tortuosity measurement by means of ultrasonic tests. In: 14th Int. Congr. Sound Vib., ICSV 2007, pp. 2132–2139, 3.

Bonfiglio, P., Pompoli, F., 2016. Frequency-dependent mechanical modelling of poro-elastic materials for sound transmission loss simulations. Noise Control Eng. J. 64 (5), 627–633.

Caniato, M., Bettarello, F., 2013. The impact of acoustics and energy efficiency protocols on comfort in the building industry. Open J. Civ. Eng. 3 (2 A), 40–45. http://dx.doi.org/10.4236/ojce.2013.32A005.

Caniato, M., A Travan, Method for recycling waste material, 2016. EP Patent 16425023.5, Trieste, Italy.

Caniato, M., Bettarello, F., Taffarel, M., 2013. Sound power level of speaking people. Proc. Mtgs. Acoust. 19, 040026. http://dx.doi.org/10.1121/1.4801052.

Caniato, M., Bettarello, F., Sbaizero, O., Schmid, C., 2015. Recycled materials for noise reduction in floating floors. In: 22nd Int. Congr. Sound Vib., ICSV 2015; Florence; Italy; 12 July 2015 through 16 July 2015. Code 121474.

Caniato, M., Bettarello, F., Marsich, L., Ferluga, A., Sbaizero, O., Schmid, C., 2016a. Time-depending performance of resilient layers under floating floors. Constr. Build. Mater. 102, 226–232. http://dx.doi.org/10.1016/j.conbuildmat.2015.10.176.

Caniato, M., Bettarello, F., Marsich, L., Ferluga, A., Sbaizero, O., Schmid, C., 2016b. Impulse response method for defect detection in polymers: description of the method and preliminary results. Polym. Test. 55, 78–87. http://dx.doi.org/10.1016/j.polymertesting.2016.08.013.

Caniato, M., Bettarello, F., Schmid, C., Fausti, P., 2016c. Assessment criterion for indoor noise disturbance in the presence of low frequency sources. App. Acoust. 113, 22–33. http://dx.doi.org/10.1016/j.apacoust.2016.06.001.

Caniato, M., Bettarello, F., Patrizio, F., Marsich, L., Ferluga, A., Schmid, C., 2016d. Low frequency noise and disturbance assessment methods: a brief literature overview and a new proposal. In: Proc. Mtgs. Acoust., 28, Article Number 032001, Incorporated in 22nd Int. Congr. Acoust.: Acoustics for the 21st Century, ICA 2016; Buenos Aires; Argentina; 5 September 2016 through 9 September 2016. http://dx.doi.org/10.1121/2.0000341.

Caniato, M., Bettarello, F., Fausti, P., Marsich, L., Ferluga, A., Schmid, C., 2017a. Impact sound of timber floors in sustainable buildings. Build. Environ. 120, 110–122. http://dx.doi.org/10.1016/j.buildenv.2017.05.015.

Caniato, M., Bettarello, F., Ferluga, A., Marsich, L., Schmid, C., Fausti, P., 2017b. Acoustic of lightweight timber buildings: a review. Renew. Sust. En. Rev. 80C, 585–596. http://dx.doi.org/10.1016/j.rser.2017.05.110.

Colombo, P., Brusatin, G., Bernardo, E., Scarinci, G., 2003. Inertization and reuse of waste materials by vitrification and fabrication of glass-based products. Curr. Opin. Solid State Mater. Sci. 7, 225–239. http://dx.doi.org/10.1016/j.cossms.2003.08.002.

Di Monte, R., Caniato, M., Boscarato, I., Kaspar, J., Sbaizero, O., 2013. Green cork-based innovative resilient and insulating materials: acoustic, thermal and mechanical characterization. In: Proc. Mtgs. Acoust. Volume 19, Article Number 040096, 6p21st Int. Congr. Acoust., ICA 2013–165th Meet. Acoust. Soc. America; Montreal, QC; Canada; 2 June 2013 through 7 June 2013. http://dx.doi.org/10.1121/1.4800619. Code 97379.

Doutres, O., Salissou, Y., Atalla, N., Panneton, R., 2010. Evaluation of the acoustic and non-acoustic properties of sound absorbing materials using a three-microphone impedance tube. Appl. Acoust. 71 (6), 506–509.

European Commission, EU Environment, 2017. ec.europa.eu/environment/circular-economy/index_en.htm. (Accessed 28 June 2017).

Fernandes, H.R., Tulyaganov, D.U., Ferreira, J.M.F., 2009. Preparation and characterization of foams from sheet glass and fly ash using carbonates as foaming agents. Ceram. Int. 35, 229–235. http://dx.doi.org/10.1016/j.ceramint.2007.10.019.

Fernandes, H.R., Ferreira, D.D., Andreola, F., Lancellotti, I., Barbieri, L., Ferreira, J.M.F., 2014. Environmental friendly management of CRT glass by foaming with waste egg shells, calcite or dolomite. Ceram. Int. 40, 13371–13379. http://dx.doi.org/10.1016/j.ceramint.2014.05.053.

Gong, Y., Dongol, R., Yatongchai, C., Wren, A.W., Sundaram, S.K., Mellott, N.P., 2016. Recycling of waste amber glass and porcine bone into fast sintered and high strength glass foams. J. Clean. Prod. 112, 4534–4539. http://dx.doi.org/10.1016/j.jclepro.2015.09.052.

Gouesbet, G., Grehan, G., 2011. Generalized Lorenz-mie Theories. Springer, Berlin.

Granzotto, N., Bettarello, F., Ferluga, A., Marsich, L., Schmid, C., Fausti, P., Caniato, M., 2017. Energy and acoustic performances of windows and their correlation. Energy Build. 136, 189–198. http://dx.doi.org/10.1016/j.enbuild.2016.12.024.

Gwon, J.G., Kim, S.K., Kim, J.H., 2016. Sound absorption behavior of flexible polyurethane foams with distinct cellular structures. Mater. Des. 89, 448–454. January 05.

Hasheminia, S., Nemati, A., Eftekhari Yekta, B., Alizadeh, P., 2012. Preparation and characterisation of diopside-based glass–ceramic foams. Ceram. Int. 38, 2005–2010. http://dx.doi.org/10.1016/j.ceramint.2011.10.035.

International Organization for Standardization (ISO), 1998. Acoustics-determination of Sound Absorption Coefficient and Impedance Tubes-part 2: Transfer-function Method. ISO 10534–2.

International Organization for Standardization (ISO), 1999. Laboratory Glassware-pyknometers. ISO 3507.

International Organization for Standardization (ISO), 2009. Particle Size Analysis-laser Diffraction Methods. ISO 13320.

Ketov, A.A., 2003. Advances in waste management and recycling. In: Proc. Int. Symp., Dundee, Scotland, pp. 695–704.

König, J., Petersen, R.R., Yue, Y., 2016. Influence of the glass particle size on the foaming process and physical characteristics of foam glasses. J. Non Cryst. Solids 447, 190–197. http://dx.doi.org/10.1016/j.jnoncrysol.2016.05.021.

Liapis, A.I., Bruttini, R., 2015. Freeze drying. In: Mujumdar, A.S. (Ed.), Handbook of Industrial Drying, , fourth ed.2015. CRC Press, Taylor & Francis Group, Boca Raton, p. 1318. ch.12, pp.259–282.

Lyttle, W.O., US patent 2,215,223, 1940. Pittsburgh Plate Glass, New Kensington,

Pennsylvania.
Marsich, E., Bellomo, F., Turco, G., Travan, A., Donati, I., Paoletti, S., 2013. Nanocompos. Scaffolds bone tissue eng. Contain. Silver nanoparticles prep. Charact. Biol. Prop. J. Mater. Sci. Mater. Med. 1799–1807. http://dx.doi.org/10.1007/s10856-013-4923-4.
Mugoni, M., Montorsi, C., Siligardi, F., Andreola, I., Lancellotti, E., Bernardo, L., Barbieri, L., 2015. Design of glass foams with low environmental impact. Ceram. Int. 41, 3400–3408. http://dx.doi.org/10.1016/j.ceramint.2014.10.127.
Omran, A., Tagnit-Hamou, A., 2016. Performance of glass-powder concrete in field applications. Constr. Build. Mater. 109, 84–95. http://dx.doi.org/10.1016/j.conbuildmat.2016.02.006.
Papadopoulos, A.M., 2005. State of the art in thermal insulation materials and aims for future developments. Energy Build. 37, 77–86. http://dx.doi.org/10.1016/j.enbuild.2004.05.006.
Parghi, M., Alam, S.M., 2016. Physical and mechanical properties of cementitious composites containing recycled glass powder (RGP) and styrene butadiene rubber (SBR). Constr. Build. Mater. 104, 34–43. http://dx.doi.org/10.1016/j.conbuildmat.2015.12.006.
Qu, Y.N., Xu, J., Su, Z.-G., Ma, N., Zhang, X.Y., Xi, X.Q., Yang, J.L., 2016. Lightweight and high-strength glass foams prepared by a novel green spheres hollowing technique. Ceram. Int. 42, 2370–2377. http://dx.doi.org/10.1016/j.ceramint.2015.10.034.
Scarinci, G., Brusatin, G., Bernardo, E., 2005. Glass foams. In: Cell. Ceram. Struct. Manuf. Prop. Appl., Scheffler M., P. Colombo, 2005, pp. 158–176.
Singh, N., Li, J., Zeng, X., 2016. Solutions and challenges in recycling waste cathode-ray tubes. J. Clean. Prod. 133, 188–200. http://dx.doi.org/10.1016/j.jclepro.2016.04.132.
Soares, J.P., Santos, J.E., Chierice, G.O., Cavalheiro, E.T.G., 2004. Thermal behavior of alginic acid and its sodium salt. Eclética Quím. 29, 57–64.
TA Instruments/Waters LLC, Misura 4.0.16 Documentation, Heating Microscope HSM, misura.readthedocs.io/en/latest/microscope/microscope.html (accessed on 21st april 2016).
Terribile, D., Llorca, J., Boaro, M., De Leitenburg, C., Dolcetti, G., Trovarelli, A., 1999. Corrigendum to: fast oxygen uptake/release over a new CeOx phase (Pg 1897, 1998). Chem. Com. 477 (5).
Travan, A., Pelillo, C., Donati, I., Marsich, E., Benincasa, M., Scarpa, T., Semeraro, S., Turco, G., Gennaro, R., Paoletti, S., 2009. Non-cytotoxic silver nanoparticle-polysaccharide nanocomposites with antimicrobial activity. Biomacromolecules 10 (6), 1429–1435. http://dx.doi.org/10.1021/bm900039x, 1429–35.
Travan, A., Scognamiglio, F., Borgogna, M., Marsich, E., Donati, I., Tarusha, L., Grassi, M., Paoletti, S., 2016. Hyaluronan delivery by polymer demixing in polysaccharide-based hydrogels and membranes for biomedical applications. Carbohydr. Polym. 2016, 408–418. http://dx.doi.org/10.1016/j.carbpol.2016.03.088.
Wu, H., Fan, J., Du, N., 2007. Thermal energy transport within porous polymer materials: effects of fiber characteristics. J. App. Polym. Sci. 106, 576–583.
Zhang, Y.S., Khademhosseini, A., 2017. Advances in engineering hydrogels. Science 356 (6337).